

Absence of ACAT-1 Attenuates Atherosclerosis but Causes Dry Eye and Cutaneous Xanthomatosis in Mice with Congenital Hyperlipidemia*

Received for publication, March 26, 2000, and in revised form, April 17, 2000
Published, JBC Papers in Press, April 20, 2000, DOI 10.1074/jbc.M002541200

Hiroaki Yagyu‡§, Tetsuya Kitamine‡§, Jun-ichi Osuga‡, Ryu-ichi Tozawa‡, Zhong Chen‡, Yuichi Kaji¶, Teruaki Oka¶, Stéphane Perrey‡, Yoshiaki Tamura‡, Ken Ohashi‡, Hiroaki Okazaki‡, Naoya Yahagi‡, Futoshi Shionoiri‡, Yoko Iizuka‡, Kenji Harada‡, Hitoshi Shimano‡, Hidetoshi Yamashita¶**, Takanari Gotoda‡, Nobuhiro Yamada‡ ‡‡, and Shun Ishibashi‡ §§

From the Departments of ‡Metabolic Diseases, ¶Ophthalmology, and ¶Pathology, Faculty of Medicine, University of Tokyo, Hongo, Tokyo 113-8655, Japan

Acyl-CoA:cholesterol acyltransferase (ACAT) catalyzes esterification of cellular cholesterol. To investigate the role of ACAT-1 in atherosclerosis, we have generated ACAT-1 null (ACAT-1^{-/-}) mice. ACAT activities were present in the liver and intestine but were completely absent in adrenal, testes, ovaries, and peritoneal macrophages in our ACAT-1^{-/-} mice. The ACAT-1^{-/-} mice had decreased openings of the eyes because of atrophy of the meibomian glands, a modified form of sebaceous glands normally expressing high ACAT activities. This phenotype is similar to dry eye syndrome in humans. To determine the role of ACAT-1 in atherogenesis, we crossed the ACAT-1^{-/-} mice with mice lacking apolipoprotein (apo) E or the low density lipoprotein receptor (LDLR), hyperlipidemic models susceptible to atherosclerosis. High fat feeding resulted in extensive cutaneous xanthomatosis with loss of hair in both ACAT-1^{-/-}:apo E^{-/-} and ACAT-1^{-/-}:LDLR^{-/-} mice. Free cholesterol content was significantly increased in their skin. Aortic fatty streak lesion size as well as cholesteryl ester content were moderately reduced in both double mutant mice compared with their respective controls. These results indicate that the local inhibition of ACAT activity in tissue macrophages is protective against cholesteryl ester accumulation but causes cutaneous xanthomatosis in mice that lack apo E or LDLR.

microsomal enzyme, acyl-CoA:cholesterol acyltransferase (ACAT; EC 2.3.1.26) (1, 2).¹ In the liver and small intestine, cholesterol is esterified by ACAT and incorporated into apolipoprotein (apo) B-containing lipoproteins, which are subsequently secreted into circulation. After lipolytic conversion, these lipoproteins are taken up by the cells of various organs, where their cholesteryl esters (CE) are hydrolyzed in lysosomes to liberate free cholesterol (FC), which is re-esterified by ACAT again for storage in cytoplasmic lipid droplets.

Two ACAT genes have been identified in mammals (3–6). ACAT-1, which was originally cloned from a macrophage cDNA library (3), is ubiquitously expressed. In particular, it is highly expressed in preputial glands, steroidogenic organs, sebaceous glands, and macrophages (7–9). However, its physiological roles in each organ are yet to be determined. ACAT-1 is also expressed in macrophage-derived foam cells in human atherosclerotic lesions (10), where it is thought to mediate foam cell formation, an initial event of atherosclerosis. Therefore, it is plausible that inhibition of ACAT in the arterial wall cells exerts a protective effect against atherosclerosis. In contrast, ACAT-2 is expressed only in the liver and small intestine and is conceivably involved in lipoprotein assembly and secretion (4–6). Consistently, ACAT activities were eliminated from the macrophages and adrenal glands but not from the liver in ACAT-1 knockout mice reported by Meiner *et al.* (11, 12).

To further explore the other unknown functions of ACAT-1 and to determine whether the elimination of ACAT-1 has an anti-atherogenic effect, we have generated ACAT-1 knockout mice by homologous recombination with a targeting vector that is designed to delete the first membrane spanning region plus a serine 268 that is crucial for the catalytic activity of ACAT-1 (13) and crossed these animals with hyperlipidemic mutant mice, apo E-deficient (apo E^{-/-}) (14), and the low density lipoprotein (LDL) receptor-deficient (LDLR^{-/-}) mice (15), which are susceptible to atherosclerosis.

MATERIALS AND METHODS

General Methods—Standard molecular biology techniques were used (16). Before sacrifice, mice were anesthetized with pentobarbital. Sick mice were euthanized. The current experiments were performed in

Esterification of intracellular cholesterol is catalyzed by a

* This work was supported by a grant-in-aid for scientific research from the Ministry of Education, Science and Culture, the Promotion of Fundamental Studies in Health Science of The Organization for Pharmaceutical Safety and Research, and Health Sciences Research grants (Research on Human Genome and Gene Therapy) from the Ministry of Health and Welfare. The costs of publication of this article were defrayed in part by the payment of page charges. This article must therefore be hereby marked "advertisement" in accordance with 18 U.S.C. Section 1734 solely to indicate this fact.

§ These authors contributed equally to this work.

** Present address: Dept. of Ophthalmology, Yamagata University School of Medicine, 2-2-2 Iidanishi, Yamagata, Yamagata 990-9585, Japan.

‡‡ Present address: Metabolism, Endocrinology, and Atherosclerosis, Inst. of Clinical Medicine, University of Tsukuba, 1-1-1 Tennodai, Tsukuba, Ibaraki 305-8575, Japan.

§§ To whom correspondence should be addressed: Dept. of Metabolic Diseases, Faculty of Medicine, University of Tokyo, 7-3-1 Hongo, Bunkyo-ku, Tokyo 113-8655, Japan. Tel.: 81-3-3815-5411 (ext. 33113); Fax: 81-3-5802-2955; E-mail: ishishash-ky@umin.ac.jp.

¹ The abbreviations used are: ACAT, Acyl-CoA:cholesterol acyltransferase; apo, apolipoprotein; LDL, low density lipoprotein; LDLR, LDL receptor; HPLC, high performance liquid chromatography; TC, total cholesterol; TG, triglycerides; FC, free cholesterol; CE, cholesteryl esters; HDL-C, cholesterol contents in high density lipoprotein fraction; kb, kilobase(s).

accord with institutional guidelines for animal experiments at the University of Tokyo.

Diets—Three diets were used: (i) a normal chow diet (MF diet from Oriental Yeast Co., Tokyo) that contained 5.6% (w/w) fat with 0.09% (w/w) cholesterol; (ii) a high fat diet A: MF diet containing 0.15% (w/w) cholesterol and 15% (w/w) butter (essentially similar to Western style diet (17)); (iii) a high fat diet B: MF diet containing 1.25% (w/w) cholesterol, 15% (w/w) cocoa butter, 0.5% (w/w) cholic acid essentially as described by Paigen *et al.* (18, 19). Preliminary experiments have shown that feeding with high fat diet B made many of the apo E^{-/-} mice sick probably because of extreme hyperlipidemia irrespective of the presence of the ACAT-1 gene. On the other hand, LDLR^{-/-} mice developed only a minimal lesions in 8 weeks when fed with high fat diet A. Accordingly, two different high fat diets were used to analyze ACAT-1^{-/-}:apo E^{-/-} or ACAT-1^{-/-}:LDLR^{-/-} double knockout mice.

Generation of ACAT-1 Knockout Mice—A fragment (1623 base pairs) of mouse ACAT-1 cDNA was amplified by polymerase chain reaction using primers that were designed based on reported sequences of human ACAT-1 cDNA (sense primer, 5'-ATGGTGGGTGAAGAGAAGATGTCTTAAGAA-3', and antisense primer, 5'-AAACACGTAACGCAAGTCCAGGAACGTGG-3') (3) and was subcloned into pCRII (Invitrogen). After labeling with ³²P using the Megaprime DNA labeling system (Amersham Pharmacia Biotech) and [α -³²P]dCTP (Amersham Pharmacia Biotech), the cDNA fragment was used as a probe to screen a 129/Sv mouse genomic library, which had been constructed in Lambda Dash II (Stratagene) as described previously (20, 21). One genomic clone coding the 5' side of ACAT-1 cDNA was sequenced. A 1-kb fragment in intron 5 was amplified by polymerase chain reaction using the following primers: sense primer, 5'-CGCTCGAGTTCAGTCTCATTAAATGAG-3' and antisense primer, 5'-CGCTCGAGGTAATTGTTCTGATGTGG-3', and used as the short arm (22). Another 13-kb genomic clone that contained a fragment of the ACAT gene spanning intron 11 to exon 16 was directly used as the long arm. A replacement-type targeting vector was constructed by ligating the short and long arms into the *Xho*I and *Not*I sites, respectively, of the vector pPollIshort-neobpA-HSVTK as described previously (15, 21) (see Fig. 1A). A 4-kb piece of the gene that contained exons 6–10, which encoded the first membrane spanning domain (23) and serine 268 that is crucial for the enzyme activity (13), was replaced by a neomycin-resistant cassette. Theoretically, homologous recombination would produce a totally inactive enzyme.

After digestion with *Sal*I, the vector was electroporated into JH1 embryonic stem cells. Targeted clones that had been selected in the presence of G418 and 1-(2-deoxy, 2-fluoro- β -D-arabinofuranosyl)-5 iodouracil were identified by polymerase chain reaction using the following primers: 5'-TCTGGAGAAAATGCAGGCTTCTTAC-3' and 5'-GATTGGGAAGACAATAGCAGGCATGC-3' (see Fig. 1A). Homologous recombination was verified by Southern blot analysis after digestion with *Eco*RI using a fragment that was upstream of the short arm as a probe (probe B; see Fig. 1A). Targeted embryonic stem clones were injected into the C57BL/6J blastocysts, yielding four lines of chimeric mice that transmitted the disrupted allele through the germline. All experiments reported here were performed with 129/Sv-C57BL/6J hybrid descendants (F1 and subsequent generations) of these animals. For genotyping, tail DNA was digested with *Bam*HI and subjected to Southern blot analyses using probe A (see Fig. 1A).

Breeding Experiments—ACAT-1^{+/-} mice were cross-bred to apo E^{-/-} or LDLR^{-/-} mice to produce mice that were heterozygous for the disrupted alleles of both ACAT-1 and either apo E or the LDL receptor loci. The intercross of these animals was performed to produce ACAT-1^{+/-}:apo E^{-/-} and ACAT-1^{+/-}:LDLR^{-/-}. Brother-sister mating of ACAT-1^{+/-}:apo E^{-/-} or ACAT-1^{+/-}:LDLR^{-/-} mice was performed to produce a set of apo E-deficient mice (ACAT-1^{+/+}:apo E^{-/-}, ACAT-1^{+/-}:apo E^{-/-}, and ACAT-1^{-/-}:apo E^{-/-}) or a set of the LDL receptor-deficient mice (ACAT-1^{+/+}:LDLR^{-/-}, ACAT-1^{+/-}:LDLR^{-/-}, and ACAT-1^{-/-}:LDLR^{-/-}), respectively. Littermates were used as controls. Therefore, genetic background of these animals were mixed: 50% C57BL/6J and 50% 129/Sv.

Preparation of Peritoneal Macrophages—Peritoneal macrophages were prepared as described previously (17).

Northern Blot Analyses—Total RNA was isolated from cultured peritoneal macrophages by using TRIZOL reagent (Life Technologies, Inc.). 10 μ g of total RNA was subjected to electrophoresis in 1% agarose gel containing formamide and transferred to a nylon filter (Hybond N, Amersham Pharmacia Biotech). cDNA probes (the 1623-base pair coding region of ACAT-1 and β -actin) were radiolabeled with [γ -³²P]dCTP. After prehybridization for 2 h, blots were hybridized in Rapidhyb^B buffer (Amersham Pharmacia Biotech) with indicated probes for 1 h at 65 °C.

Immunoblot Analyses—cDNA fragment encoding N-terminal 125

amino acids of ACAT-1 was amplified by polymerase chain reaction using primers (sense primer, 5'-GAGCATATGCTACTAAGAAACCGGCTGTCA-3'; antisense primer, 5'-TTCGGATCCCTTAGTCTAAAAAGAGACTGCCT-3') and cDNA pool made from mouse peritoneal macrophages and subcloned into the expression vector PW6A (24). After transformation, *Escherichia coli*, BL21(DE3), were grown in LB medium in the presence of isopropyl- β -D-thiogalactopyranoside. The cells were disrupted by sonication and centrifuged to remove cellular debris. The recombinant ACAT-1 peptide was purified by chromatography using SP Sepharose FF column followed by Superdex 75 columns. ACAT-1^{-/-} mice were immunized with the purified recombinant ACAT-1 peptide. Standard technique was used to generate a monoclonal antibody (25).

Peritoneal macrophages (1×10^7 cells) were resuspended in 100 μ l of buffer A (50 mM Tris-HCl, pH 7.8, 5 mM EDTA, 0.1 mM phenylmethylsulfonyl fluoride) containing 5% SDS. After an overnight incubation at 4 °C, 50 μ g of protein was subjected to SDS/polyacrylamide gel electrophoresis. After transfer to a nitrocellulose membrane, immunoblot was performed using an ECL kit (Amersham Pharmacia Biotech) with anti-mouse IgG (Amersham Pharmacia Biotech) as the secondary antibody.

Plasma Lipoprotein Analyses—After a 16-h fast, blood was collected from the retro-orbital venous plexus into tubes containing EDTA. Plasma levels of total cholesterol (TC) and triglycerides (TG) were determined enzymatically using kits (Determiner TC555 and Determiner TG555, Kyowa Medex). Lipoproteins were fractionated by high performance chromatography (HPLC), and the cholesterol contents in high density lipoprotein fraction (HDL-C) were determined as described (17).

Tissue and Cellular Lipids—Lipids were extracted from tissues by the method of Folch *et al.* (26). TC and FC were determined by fluorometric microassay according to a modified method of Heider and Boyett (27) with the exception that 0.01% (v/v) Triton X-100 was used instead of Carbowax-600.

Assay of ACAT Activity—Tissue was homogenized in buffer B (0.25 M sucrose, 1 mM EDTA, 2 μ g/ml leupeptin, and 50 mM Tris-HCl, pH 7.0) and centrifuged at $107,000 \times g$ for 60 min at 4 °C. The pellets were resuspended and used for the assay. ACAT activity in microsomes or cell homogenates was determined by the rate of incorporation of [¹⁴C] oleoyl-CoA into the CE fraction according to Billheimer *et al.* with minor modifications (28, 29).

Histology—Tissues were fixed with neutral-buffered formalin, embedded in paraffin, and stained with hematoxylin and eosin. The aortic cross-sectional lesion area was evaluated according to a modified method of Paigen *et al.* (17, 30). In brief, the hearts were perfused with saline containing 4% (w/v) formalin and fixed for more than 48 h in the same solution. The basal half of the hearts was embedded in Tissue-Tek OCT compound (Miles, Inc.), and the serial sections were captured using Cryostat microtome (6- μ m thick) as described (31). Four sections, each separated by 60 μ m, were used to evaluate the lesions: two at the end of the aortic sinus and two at the junctional site of sinus and ascending aorta. The sections were stained with Oil Red O and counterstained with hematoxylin.

Statistics—Data are represented as the means \pm S.D. Student's *t* test and analysis of variance were used to compare the mean values between two and three groups, respectively.

RESULTS

Tissue-specific Role of ACAT-1—A replacement-type vector was used to generate chimeric mice (Fig. 1A). Heterozygous ACAT-1 knockout mice (ACAT-1^{+/-}) born by these chimera, which were viable and fertile, were intercrossed to obtain homozygous ACAT-1 knockout mice (ACAT-1^{-/-}). Wild type, heterozygotes, and homozygotes were born in accordance with Mendelian fashion (+/+ : +/+ : -/- = 17:40:19, $\chi^2 = 0.16$; *p* = 0.92) (Fig. 1B).

To determine whether the expression of the ACAT-1 gene was ablated, we performed Northern blot analyses (Fig. 1C). Although three major mRNA transcripts (9.0, 4.6, and 3.5 kb) were detectable in wild-type macrophages, adrenal glands, ovaries, and testes, no bands were detectable in these organs from ACAT-1^{-/-} mice. Approximately one-half of the amounts of the three transcripts were expressed by the cells from ACAT-1^{+/-} mice. Consistent with the Northern blot results, immunoblot analyses revealed no proteins that were immunoreactive with an antibody raised against recombinant mouse ACAT-1 in the peritoneal macrophages (Fig. 1D), adrenal glands, ovaries,

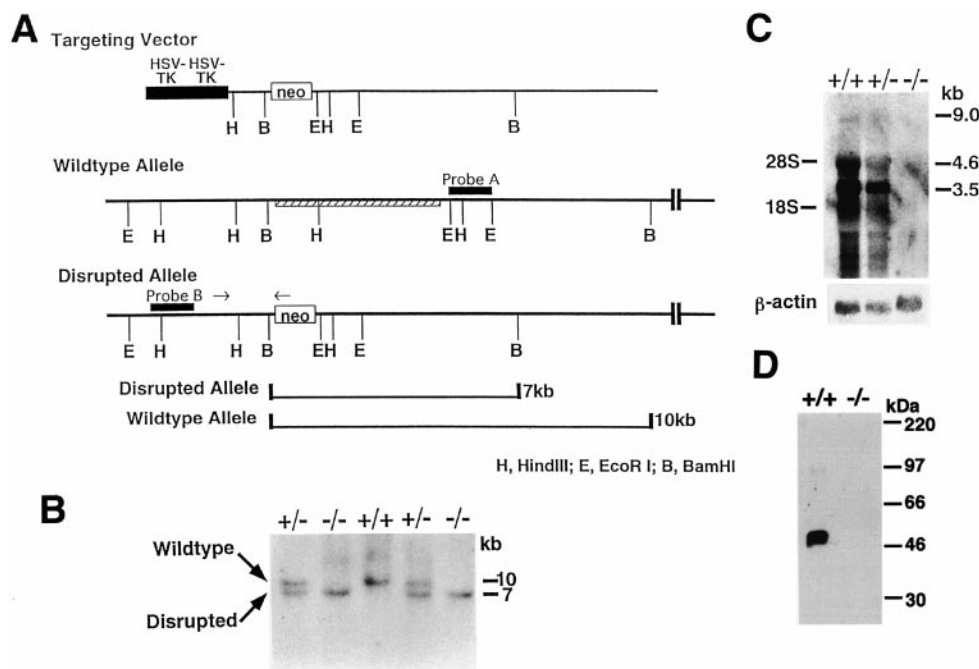


FIG. 1. Targeted disruption of the ACAT-1 gene. *A*, a map of the ACAT-1 locus, together with the sequence replacement gene-targeting vector and the targeted ACAT-1 allele. The gene targeting event replaced a 4-kb fragment containing the first transmembrane domain and a conserved serine with a cassette containing a neomycin-resistance gene (*neo*^r) driven by the RNA polymerase II promoter. Two copies of herpes simplex virus thymidine kinase (*HSV-TK*) expression cassette were used as a negative selection marker. Gene-targeting events were verified by Southern blot analyses using *Eco*RI and probe B for embryonic stem cell DNA and *Bam*HI and probe A for tail DNA. *B*, Southern blot of *Bam*HI fragment in the targeted allele is 7 kb versus 10 kb for the wild-type allele when hybridized with probe A. DNA was isolated from tails of offspring of heterozygous matings. *C*, Northern blot analyses. 10 μ g of total RNA was isolated from peritoneal macrophages in culture and subjected to Northern blot analyses. Two probes were used: cDNA fragment containing the entire coding region of ACAT-1 (1623 base pairs) and β -actin as a reference. Three major transcripts are indicated. *D*, immunoblot analyses. Peritoneal macrophages were isolated, and 50 μ g of cellular protein was subjected to SDS/polyacrylamide gel electrophoresis. After transfer to a nitrocellulose membrane, immunoblot was performed using an ECL kit with the antibody against a recombinant peptide encoding N-terminal 125 amino acids of ACAT-1 and anti-mouse IgG as the secondary antibody.

and testes. Therefore, it is reasonable to conclude that our ACAT-1^{-/-} mice were virtually null for ACAT-1.

Table I compares ACAT activities in microsomes prepared from the liver, small intestine, adrenal glands, testes, and ovaries, between the wild-type and ACAT-1^{-/-} mice. In ACAT-1^{-/-} mice, ACAT activity was barely detectable in the adrenal glands, testes, and ovaries that normally express substantial ACAT activity in the wild-type mice. In contrast to these steroidogenic organs, the liver and small intestine from the ACAT-1^{-/-} mice expressed ACAT activities similar to those from wild-type mice.

Atrophy of Meibomian Gland—ACAT-1^{-/-} mice were grossly normal except that they had narrow eye fissures and lipid-depleted adrenal glands. Abnormal facial expression was noted around the weaning age (3–4 weeks) in almost all ACAT-1^{-/-} mice (Fig. 2). Pathological examination of the eye balls and adnexa revealed that ACAT-1^{-/-} mice had atrophic acinar cells in the meibomian glands (Fig. 2). Upon bio-microscopic examination, fine punctate stripping of the corneal epithelium was observed. No other abnormalities were found in conjunctiva, cornea, retina, or Harderian glands. Lipids in adrenal cortex were depleted in ACAT-1^{-/-} mice (data not shown).

We measured FC and CE contents in steroidogenic organs whose ACAT activities were markedly reduced in ACAT-1^{-/-} mice and meibomian glands that exhibited remarkable acinar cell shrinkage in ACAT-1^{-/-} mice (Fig. 3). In wild-type mice, most of cholesterol was stored in its esterified form in adrenal glands, ovaries, and meibomian glands. CE contents of these organs were markedly reduced to a base-line level in ACAT-1^{-/-} mice. Interestingly, FC content was increased only in the meibomian glands of ACAT-1^{-/-} mice. There were virtually no

TABLE I
Microsomal ACAT activities in various organs of wild-type and ACAT-1^{-/-} mice

Microsomes were prepared from the indicated organs of wild-type (+/+) and ACAT-1^{-/-} (-/-) mice aged 3 months. ACAT activities were measured as described under "Materials and Methods."

Tissue	ACAT	n	ACAT activity pmol/mg/min
Liver	+/+	3	156 ± 20
	-/-	3	139 ± 36
Small intestine	+/+	2	111
	-/-	2	221
Adrenal	+/+	3 ^a	286
	-/-	3 ^a	<5
Testis	+/+	1	192
	-/-	1	<5
Ovary	+/+	2 ^a	2330
	-/-	2 ^a	23

^a The assay was performed on pooled samples from the indicated number of animals. Data represent the means ± S.D.

differences in CE content of testes between wild-type and ACAT-1^{-/-} mice.

Massive Cutaneous Xanthomatosis and Alopecia in ACAT-1^{-/-} Mice Lacking apo E or the LDL Receptor—To determine whether hyperlipidemia affects the phenotypes of ACAT-1^{-/-} mice, we generated mice lacking both ACAT-1 and either apo E (ACAT-1^{-/-}:apo E^{-/-}) or LDL receptor (ACAT-1^{-/-}:LDLR^{-/-}) by cross-breeding and used their littermates as controls. Although the inactivation of the ACAT-1 gene did not have a significant effect on the lipoprotein profiles in apo E^{-/-} mice, it slightly increased intermediate density lipoprotein/LDL cholesterol levels in LDLR^{-/-} mice (Table II). These

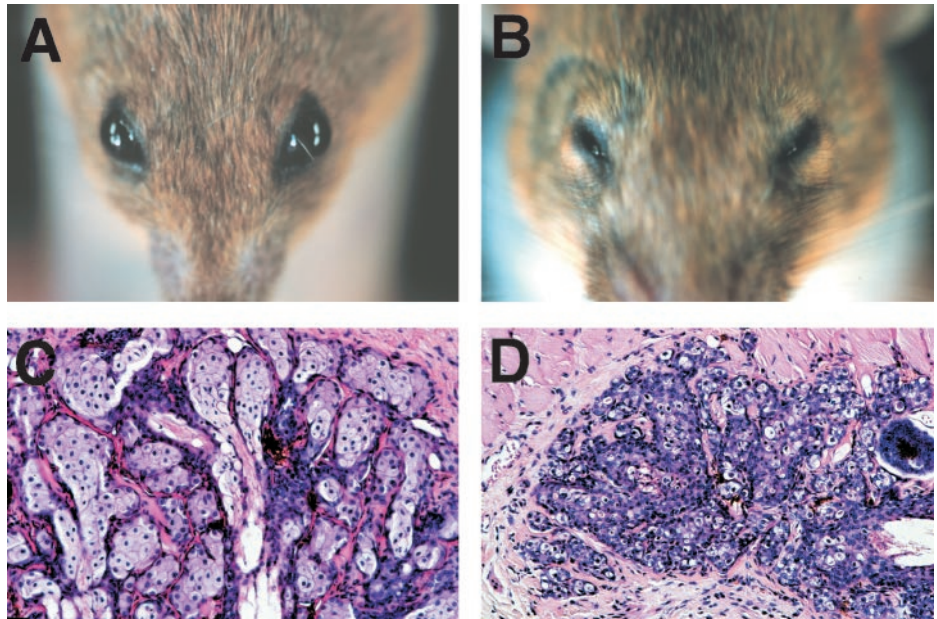


FIG. 2. Facial appearance and histology of meibomian glands of wild-type (+/+) and ACAT-1^{-/-} (-/-) mice. Facial appearance (A, +/+; B, -/-) and histology of meibomian glands (C, +/+; D, -/-) are shown. Tarsus was prepared from eyelids and used for histological examination (hematoxylin and eosin staining). The mice were females aged 5 months. Note the narrow eye fissures and atrophic meibomian glands in ACAT-1^{-/-} mice.

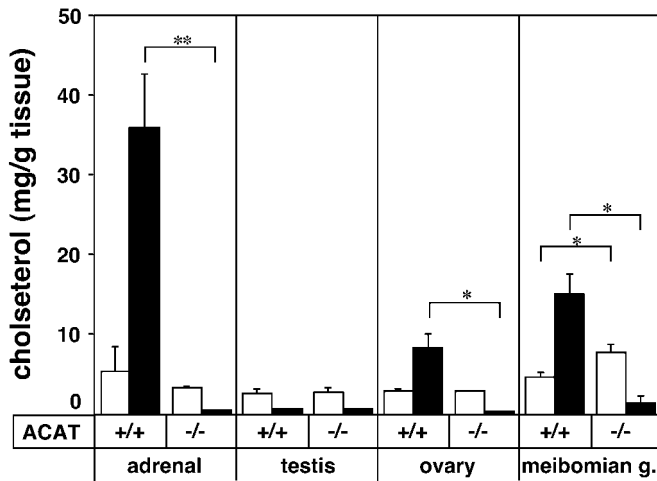


FIG. 3. FC and CE contents of adrenal glands, testes, ovaries and meibomian glands. Open bars represent FC, and closed bars represent CE. Lipids were extracted by Folch's method and quantitated by the fluorometric assay. Three mice aged 5 months were used. *, $p < 0.01$; **, $p < 0.001$ versus +/+. Significant reduction in CE was noted in the adrenals, ovaries, and meibomian glands. FC was increased only in the meibomian glands of ACAT-1^{-/-} mice.

hyperlipidemic mice lacking the ACAT gene developed skin lesions upon aging (Fig. 4). Even on a normal chow diet, about 20% of ACAT-1^{-/-}:apo E^{-/-} mice developed skin lesions by the age of 6 months (Fig. 4C). Typically, hair was lost, and skin became rough and thick. In contrast, ACAT-1^{-/-}:LDLR^{-/-} mice did not develop obvious skin lesions, at least by the age of 6 months, as long as they were maintained on a normal chow diet.

When ACAT-1^{-/-}:apo E^{-/-} and ACAT-1^{-/-}:LDLR^{-/-} mice were fed high fat diets A and B, respectively, both mice developed more pronounced hypercholesterolemia (Table II) and more extensive skin lesions (Fig. 4D). Compared with ACAT-1^{+/+}:apo E^{-/-} mice, ACAT-1^{-/-}:apo E^{-/-} mice had a 42% decrease in very LDL/intermediate density lipoprotein-cholesterol levels. There was no difference in the plasma lipoprotein profiles between ACAT-1^{+/+}:LDLR^{-/-} and ACAT-1^{-/-}:LDLR^{-/-} mice, whereas very LDL/intermediate density lipoprotein/LDL-cholesterol levels were increased in ACAT-1^{+/+}:LDLR^{-/-} mice by 22%.

Microscopic examination revealed extensive infiltration of

macrophages throughout the entire dermal layer of ACAT-1^{-/-}:apo E^{-/-} and ACAT-1^{-/-}:LDLR^{-/-} mice fed the high fat diets (Fig. 5, C and D). Many macrophages exhibited foamy appearance with multiple nuclei similar to the Touton type giant cells (Fig. 5, E and F). The thickened dermis was also filled with necrotic acellular areas containing cholesterol clefts (Fig. 5). The number of hair follicles was remarkably reduced. It is noteworthy that subcutaneous adipose tissues, which were normally present in mice with ACAT-1 gene (Fig. 5, A and B), were not discernible in the hyperlipidemic ACAT-1^{-/-} mice. Measurements of FC and CE contents of the xanthomatous skins showed that FC content was specifically increased by 5.5-fold in ACAT-1^{-/-}:apo E^{-/-} (20.0 ± 14.8 versus 3.7 ± 1.5 $\mu\text{g}/\text{mg}$ tissue; $n = 3$) and 9.7-fold in ACAT-1^{-/-}:LDLR^{-/-} mice (31.0 ± 19.6 versus 3.2 ± 1.1 $\mu\text{g}/\text{mg}$ tissue; $p < 0.05$, $n = 3$).

Moderate Suppression of Diet-induced Atherosclerosis in ACAT-1^{-/-} Mice Lacking apo E or the LDL Receptor—After feeding the sets of apo E and the LDL receptor-deficient mice with high fat diets A and B, respectively, for 8 weeks, atherosclerotic lesion size was evaluated at the aortic roots (Fig. 6). ACAT-1^{-/-}:apo E^{-/-} mice developed a 33% smaller lesion area than ACAT-1^{+/+}:apo E^{-/-} mice. ACAT-1^{-/-}:LDLR^{-/-} mice had a 53% reduction in lesion area compared with ACAT-1^{+/+}:LDLR^{-/-} mice. There were no significant differences in the lesion size between males and females in each genotype. With regard to the aortic CE contents, 3-fold and 2-fold decreases were observed in ACAT-1^{-/-}:apo E^{-/-} mice and ACAT-1^{-/-}:LDLR^{-/-} mice, respectively, as compared with their ACAT-1^{+/+} controls (Fig. 7). In contrast to cutaneous xanthomas, aortic FC contents were not increased.

DISCUSSION

In the present study, we have established ACAT-1 null mice and shown that ACAT-1 is involved in meibomian gland function, xanthoma formation, and atherosclerosis development in hyperlipidemic mouse models. Previously, Meiner *et al.* (11) disrupted the ACAT-1 gene in mice. They reported that their ACAT-1 knockout mice showed significant decreases in cholesterol esterification in embryonic fibroblasts and adrenal membranes. Although these ACAT-1^{-/-} mice had adrenal lipid depletion and decreased CE content in peritoneal macrophages, the liver retained significant cholesterol esterification activity, suggesting that cholesterol esterification involves more than one form of esterification enzyme. In addition to

TABLE II
Effects of the high fat diet feeding on the plasma lipid levels of ACAT-1^{-/-} mice lacking either apo E or LDL receptor

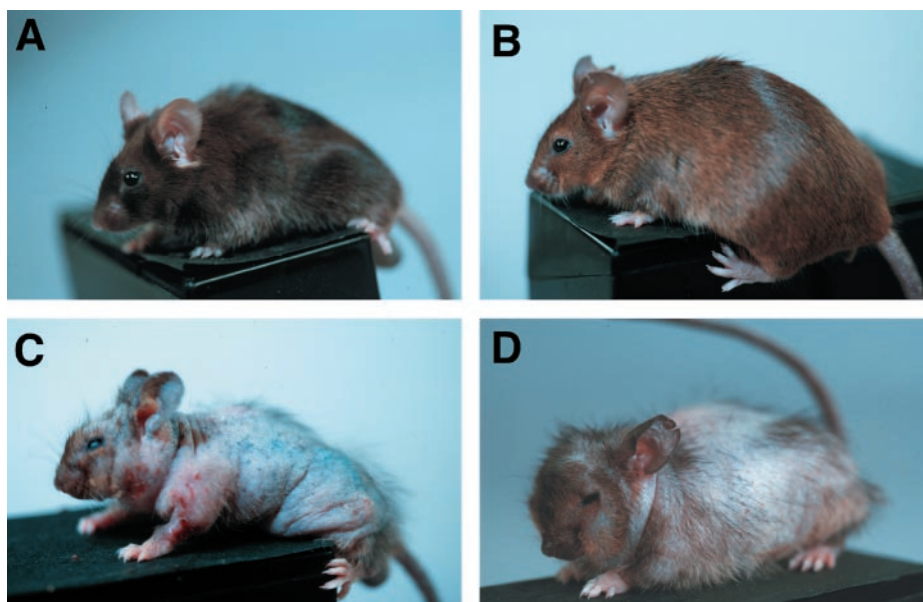
At the age of 3 months, apo E-deficient mice were fed high fat diet A, and LDL receptor-deficient mice were fed high fat diet B. Blood was taken before and after feeding for 8 weeks. HDL-C was determined by HPLC using pooled plasma. TC, TG, and HDL-C are in mg/dl. Data represent the means \pm S.D.

Genotype	Diet		ACAT-1 ^{+/+} 10 (5, 5)	ACAT-1 ^{+/-} 10 (4, 6)	ACAT-1 ^{-/-} 9 (5, 4)
Apo E ^{-/-}	Normal diet	TC	777 \pm 236	837 \pm 392	573 \pm 163
		TG	133 \pm 32	134 \pm 32	142 \pm 47
		HDL-C	9	9	9
	High fat diet A	TC	1471 \pm 472	1202 \pm 572	857 \pm 157 ^a
		TG	181 \pm 86	152 \pm 52	156 \pm 52
		HDL-C	11	8	10
			10 (5, 5)	9 (4, 5)	8 (3, 5)
LDLR ^{-/-}	Normal diet	TC	254 \pm 42	292 \pm 48	308 \pm 45 ^b
		TG	191 \pm 70	203 \pm 63	279 \pm 107 ^b
		HDL-C	149	136	168
	High fat diet B	TC	1918 \pm 453	2334 \pm 308 ^b	2045 \pm 297
		TG	141 \pm 89	145 \pm 79	140 \pm 44
		HDL-C	14	16	20

^a $p < 0.01$ versus ACAT-1^{+/+} mice by analysis of variance.

^b $p < 0.05$ versus ACAT-1^{+/+}.

FIG. 4. Cutaneous xanthomatosis and alopecia in ACAT-1-deficient mice that also lacked either apo E or the LDL receptor. No apparent skin lesions were observed in ACAT-1^{+/+}:apo E^{-/-} (A) and ACAT-1^{+/+}:LDLR^{-/-} mice (B). ACAT-1^{-/-}:apoE^{-/-} (C) and ACAT-1^{-/-}:LDLR^{-/-} mice (D) developed generalized alopecia with scaly thickened skin. ACAT-1^{+/+}:apo E^{-/-} and ACAT-1^{-/-}:apo E^{-/-} mice were 7-month-old males fed a normal chow diet. ACAT-1^{+/+}:LDLR^{-/-} and ACAT-1^{-/-}:LDLR^{-/-} mice were 5-month-old females fed the high fat diet B for 8 weeks.



confirming Meiner's original observations, we found that cholesterol esterification in the epithelium of small intestine is not mediated by ACAT-1. This is in agreement with the observations that wild-type small intestine expresses negligible amounts of ACAT-1 (7, 8) and that human intestinal ACAT activity is largely resistant to immunodepletion with an antibody against ACAT-1 (32). Recently, three groups independently reported that a second gene product (ACAT-2) is exclusively expressed in the small intestine and liver in both nonhuman primates and mice (4–6). Therefore, ACAT-2 appears to mediate the formation of the CE that is used for lipoprotein assembly and secretion.

Unexpectedly, we noticed that our ACAT-1^{-/-} mice had altered facial appearance mainly because of narrow eye fissures (Fig. 2). This phenotype was noticeable as early as 3 weeks old and had almost complete penetrance. It can result from either palpebral edema, buphthalmos, corneal diseases, impaired sight, reduction in retro-orbital tissue mass, etc. We found no abnormalities except for corneal erosion probably because of atrophic meibomian glands (Fig. 2). Therefore, dysfunction of meibomian glands may account for the narrow eye fissures. Consistently, ACAT-1 is highly expressed in meibo-

mian glands (data not shown). The meibomian dysfunction may result from reduced amounts of CE, increases in FC, or both (Fig. 3). Meibomian gland dysfunction may cause a decrease in the superficial lipid layer of tear film, thereby increasing the evaporation of aqueous component of the tear. This condition is similar to dry eye syndrome in humans (33). In this context, it is interesting to note that meibomian glands are modified sebaceous glands which also express high levels of ACAT-1 (8). In addition, we observed atrophic sebaceous glands in ACAT-1^{-/-} mice, but the penetrance of this phenotype was not complete. Atrophy of sebaceous glands has been reported in cynomolgus monkeys treated with an ACAT inhibitor, PD 132301-2 (34). Clinically, meibomian and sebaceous glands are commonly affected together; keratoconjunctivitis is frequently associated with sebaceous gland diseases such as seborrhea sicca (35). Further studies will be needed to determine whether abnormal ACAT-1 underlies these diseases.

Jong *et al.* (36) have recently described cutaneous abnormalities including atrophy of both sebaceous and meibomian glands in transgenic mice overexpressing apo CI. Because FC is increased in the skin of the apo CI transgenic mice, the overexpressed apo CI may inhibit ACAT activities in the glands,

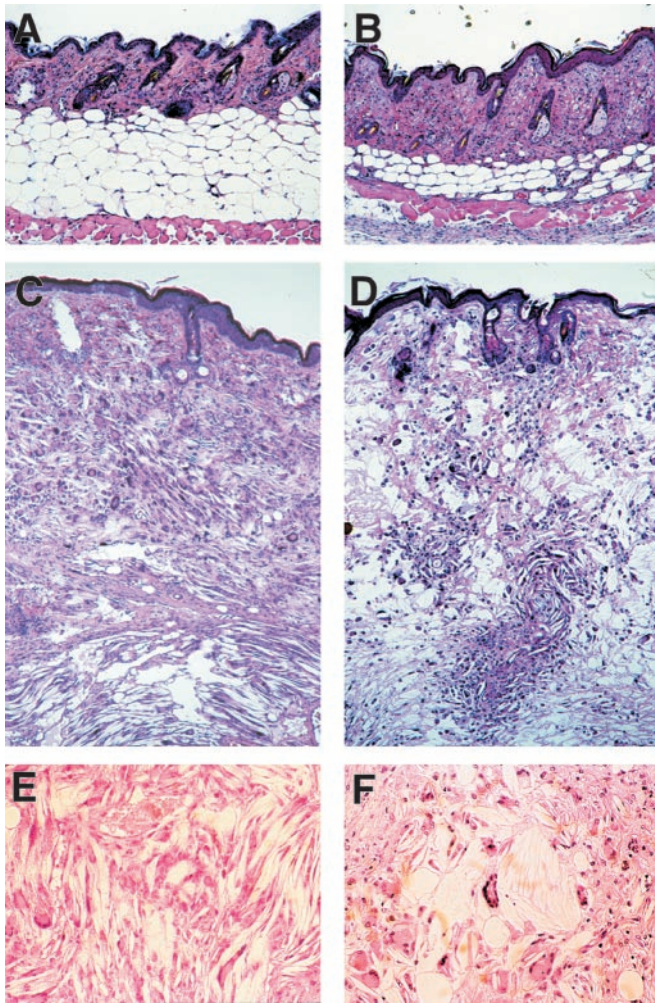


FIG. 5. Histopathology of cutaneous lesions developed in ACAT-1^{-/-}:apo E^{-/-} and ACAT-1^{-/-}:LDLR^{-/-} mice fed the high fat diets. 3-month-old mice were used for experiments of high fat feeding. ACAT-1^{+/+}:apo E^{-/-} and ACAT-1^{-/-}:apo E^{-/-} mice were fed high fat diet A for 8 weeks; ACAT-1^{+/+}:LDLR^{-/-} and ACAT-1^{-/-}:LDLR^{-/-} mice were fed high fat diet B for 8 weeks. ACAT-1^{+/+}:apo E^{-/-} (A) and ACAT-1^{+/+}:LDLR^{-/-} mice (B) had normal epidermal and dermal structure with substantial subcutaneous adipose tissue. No foam cells were observed. In ACAT-1^{-/-}:apo E^{-/-} (C and D) and ACAT-1^{-/-}:LDLR^{-/-} mice (D and F), the dermal layers were extensively infiltrated with fat-laden macrophage (foam cells). Acellular necrotic areas with cholesterol clefts were present. There were a reduced number of hair follicles. Note that subcutaneous adipose tissue was not discernible. High magnification of the dermal layer of ACAT-1^{-/-}:apo E^{-/-} (E) and ACAT-1^{-/-}:LDLR^{-/-} mice (F) is shown. Many macrophages exhibited multinucleated giant cell appearance with eosinophilic cytoplasm.

thereby producing phenotypes similar to those of our ACAT-1^{-/-} mice. Phenotypic similarity to the mutant mouse *asebia* (*ab*) was discussed in their paper (37). Recently, Zheng *et al.* (38) have reported that the stearoyl-CoA desaturates 1 (*Scd1*) gene is disrupted in the *ab* mice. Because *Scd1* catalyzes the formation of monounsaturated fatty acids, it is tempting to speculate that cholesterol esterified with monounsaturated fatty acids is required for normal meibomian function. Further studies are needed to clarify this intriguing issue.

The most outstanding phenotype observed in this study was cutaneous xanthomatosis with generalized alopecia in the double mutant mice (Figs. 4 and 5). Hair loss may be secondary to the severe xanthomatosis; however, the LDL receptor knockout mice fed an atherogenic diet develop massive xanthomatosis but not alopecia (19). Therefore, xanthomatosis and alopecia may be independent of each other. Here again, the alopecia

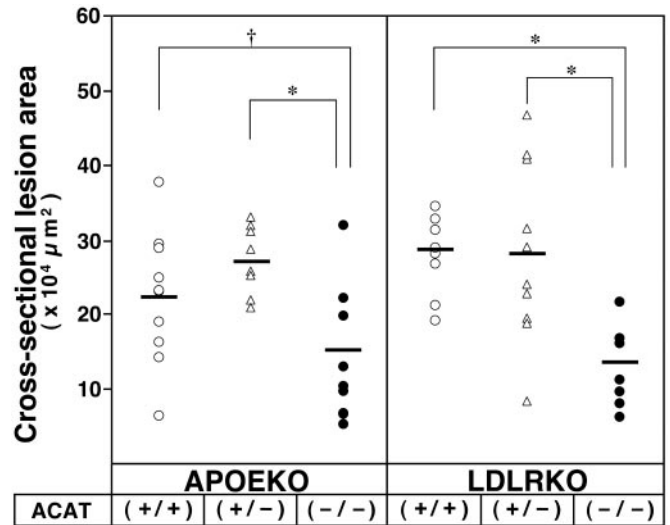


FIG. 6. Effects of the inactivation of the ACAT-1 gene on atherosclerotic plaque size. 3-month-old mice were used for experiments of high fat feeding. Apo E^{-/-} mice were fed high fat diet A for 8 weeks, and LDLR^{-/-} mice were fed high fat diet B for 8 weeks. 10 ACAT-1^{+/+}:apo E^{-/-} (5 males and 5 females), 10 ACAT-1^{+/-}:apo E^{-/-} (4 males and 6 females), and 9 ACAT-1^{-/-}:apo E^{-/-} mice (5 males and 4 females) were fed high fat diet A for 8 weeks. Ten ACAT-1^{+/+}:LDLR^{-/-} (5 males and 5 females), 9 ACAT-1^{+/-}:LDLR^{-/-} (4 males and 5 females), and 8 ACAT-1^{-/-}:LDLR^{-/-} mice (3 males and 5 females) were fed high fat diet B for 8 weeks. Plasma lipoprotein profiles are shown in Table II. After feeding with the high fat diets for 8 weeks, cross-sectional lesion areas were evaluated in the aortic roots of the mice. †, *p* < 0.05; *, *p* < 0.01 by analysis of variance.

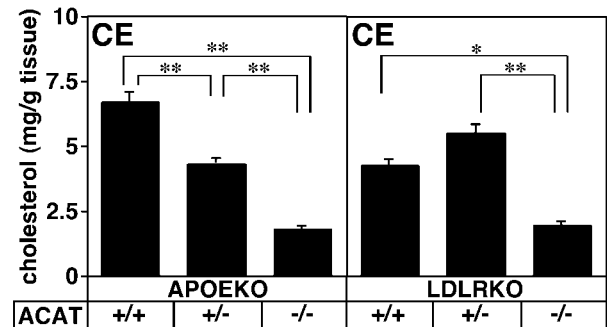
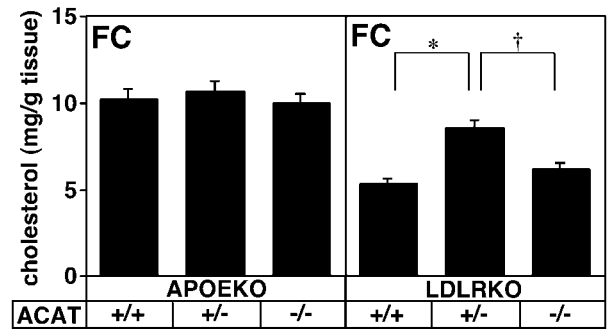


FIG. 7. Cholesterol content of the aorta. 3-month-old mice were used for experiments of high fat feeding. Apo E^{-/-} mice were fed high fat diet A for 8 weeks, and LDLR^{-/-} mice were fed high fat diet B for 8 weeks. Aortas were prepared from the same animals that were used for the evaluation of atherosclerotic lesion sizes as shown in Fig. 6. Attached connective tissue and fat were removed from the aorta as much as possible. Lipids were extracted, and TC and FC content was measured. CE content was obtained by subtracting FC from TC. Results for FC and CE are shown in the upper and lower panels, respectively. There were significant decreases in the CE content of the aortas from mice lacking ACAT-1 as compared with those from mice with ACAT-1. †, *p* < 0.05; *, *p* < 0.01; **, *p* < 0.001 by analysis of variance.

developed in apo CI transgenic mice may be relevant; apo CI transgenics have atrophic sebaceous glands, infiltration of inflammatory cells, and a hairless coat (36). Because ACAT-1 is highly expressed in sebaceous glands (8), it is reasonable to assume that ACAT-1 deficiency causes atrophy of these glands as it does in meibomian glands resulting in reduced sebaceous outflow of sebum onto the skin. Indeed, some, but not all, sebaceous glands showed atrophic changes in ACAT-1^{-/-} mice (data not shown). There was massive accumulation of FC in the cutaneous xanthomas, as evidenced histologically by the presence of cholesterol clefts. Probably, plasma lipoproteins are taken up by macrophages in which their CE are hydrolyzed but are not re-esterified because of the absence of ACAT-1. This may lead to an unlimited increase in cellular FC, which may eventually result in cell death (39). The presence of giant multinucleated cells indicates the inflammatory nature of the lesions. At present, we are unaware of a human disease which parallels this skin lesion. Common pathogenesis may underlie certain types of non-X histiocytosis such as xanthoma disseminatum or necrobiotic xanthogranuloma (40). Absence of subcutaneous fats may reflect the wasting nature of the disease. Alternatively, the adipose tissue may be destroyed by infiltrating inflammatory cells.

The effects of ACAT-1 deficiency on atherosclerosis are interesting. Several ACAT inhibitors reduced plasma lipids by suppressing lipoprotein production in the liver and intestine (41). In addition to the hypolipemic effects, these compounds are expected to reduce foam cell formation in atherosclerotic lesions, thereby inhibiting the progression of atherosclerosis *in situ* (42). As expected, CE accumulation was markedly reduced by ACAT-1 disruption in the settings of both apo E and the LDL receptor deficiency (Fig. 7). However, the effects on the atherosclerotic lesion size appeared more moderate compared with those on CE contents. Because Oil-Red-O stains only neutral lipids, the staining could potentially underestimate the lesion size in the animals that lacked CE formation. In the setting of apo E deficiency, the mean cross-sectional lesion size was reduced by 30%. This anti-atherogenic effect may be accounted for simply by the reduction of the plasma TC levels, because the plasma TC levels were reduced by 40% in ACAT-1^{-/-}:apoE^{-/-} mice compared with in ACAT-1^{+/+}:apoE^{-/-} mice.

In the setting of the LDL receptor deficiency, a similar degree of suppression in atherosclerotic lesions was observed despite the fact that the plasma TC levels were not reduced. In this particular model, it is reasonable to speculate that local inhibition of ACAT activity results in reduction in atherosclerosis. Therefore, it may be important to take background clinical condition into account, when treating atherosclerosis with ACAT inhibitors.

During the preparation of this manuscript, Accad *et al.* (43) published a report on atherosclerosis and cutaneous xanthomatosis of mice lacking both ACAT-1 and either apo E or the LDL receptor. Their observations are essentially similar to ours; however, they did not provide quantitative results of the lesion size and CE contents of the aortas. Instead, they performed more detailed histological analyses of the lesions and found paucity of macrophage-derived foam cells in the lesions from mice lacking ACAT-1.

In conclusion, the current study reveals that ACAT-1 is required for normal meibomian function. Inhibition of ACAT-1 is useful to prevent the CE accumulation in atherosclerotic lesions that develop in the hyperlipidemic state. However, exacerbation of xanthomas is a potential complication of therapy with ACAT inhibitors.

Acknowledgment—We thank A. H. Hasty for critical reading of the manuscript.

REFERENCES

- Goodman, D. S. (1965) *Physiol. Rev.* **45**, 747–839
- Suckling, K. E., and Stange, E. F. (1985) *J. Lipid. Res.* **26**, 647–671
- Chang, C. C., Huh, H. Y., Cadigan, K. M., and Chang, T. Y. (1993) *J. Biol. Chem.* **268**, 20747–20755
- Anderson, R. A., Joyce, C., Davis, M., Reagan, J. W., Clark, M., Shelness, G. S., and Rudel, L. L. (1998) *J. Biol. Chem.* **273**, 26747–26754
- Cases, S., Novak, S., Zheng, Y. W., Myers, H. M., Lear, S. R., Sande, E., Welch, C. B., Lusis, A. J., Spencer, T. A., Krause, B. R., Erickson, S. K., and Farese, R. V., Jr. (1998) *J. Biol. Chem.* **273**, 26755–26764
- Oelkers, P., Behari, A., Cromley, D., Billheimer, J. T., and Sturley, S. L. (1998) *J. Biol. Chem.* **273**, 26765–26771
- Uelmen, P. J., Oka, K., Sullivan, M., Chang, C. C. Y., Chang, T. Y., and Chan, L. (1995) *J. Biol. Chem.* **270**, 26192–26201
- Meiner, V., Tam, C., Gunn, M. D., Dong, L. M., Weisgraber, K. H., Novak, S., Myers, H. M., Erickson, S. K., and Farese, R. V., Jr. (1997) *J. Lipid. Res.* **38**, 1928–1933
- Chang, T. Y., Chang, C. C., and Cheng, D. (1997) *Annu. Rev. Biochem.* **66**, 613–638
- Miyazaki, A., Sakashita, N., Lee, O., Takahashi, K., Horiuchi, S., Hakamata, H., Morganelli, P. M., Chang, C. C., and Chang, T. Y. (1998) *Arterioscler. Thromb. Vasc. Biol.* **18**, 1568–1574
- Meiner, V. L., Cases, S., Myers, H. M., Sande, E. R., Bellosta, S., Schambelan, M., Pitas, R. E., McGuire, J., Herz, J., and Farese, R. V., Jr. (1996) *Proc. Natl. Acad. Sci. U. S. A.* **93**, 14041–14046
- Joyce, C., Skinner, K., Anderson, R. A., and Rudel, L. L. (1999) *Curr. Opin. Lipidol.* **10**, 89–95
- Cao, G., Goldstein, J. L., and Brown, M. S. (1996) *J. Biol. Chem.* **271**, 14642–14648
- Zhang, S. H., Reddick, R. L., Piedrahita, J. A., and Maeda, N. (1992) *Science* **258**, 468–471
- Ishibashi, S., Brown, M. S., Goldstein, J. L., Gerard, R. D., Hammer, R. E., and Herz, J. (1993) *J. Clin. Invest.* **92**, 883–893
- Sambrook, J., Fritsch, E. F., and Maniatis, T. (1989) *Molecular Cloning: A Laboratory Manual*, Cold Spring Harbor Laboratory, Cold Spring Harbor, NY
- Yagyu, H., Ishibashi, S., Chen, Z., Osuga, J., Okazaki, M., Perrey, S., Kitamine, T., Shimada, M., Ohashi, K., Harada, K., Shionoiri, F., Yahagi, N., Gotoda, T., Yazaki, Y., and Yamada, N. (1999) *J. Lipid. Res.* **40**, 1677–1685
- Paigen, B., Morrow, A., Brandon, C., Mitchell, D., and Holmes, P. (1985) *Atherosclerosis* **57**, 65–73
- Ishibashi, S., Goldstein, J. L., Brown, M. S., Herz, J., and Burns, D. K. (1994) *J. Clin. Invest.* **93**, 1885–1893
- Osuga, J., Inaba, T., Harada, K., Yagyu, H., Shimada, M., Yazaki, Y., Yamada, N., and Ishibashi, S. (1995) *Biochem. Biophys. Res. Commun.* **214**, 653–662
- Tozawa, R., Ishibashi, S., Osuga, J., Yagyu, H., Oka, T., Chen, Z., Ohashi, K., Perrey, S., Shionoiri, F., Yahagi, N., Harada, K., Gotoda, T., Yazaki, Y., and Yamada, N. (1999) *J. Biol. Chem.* **274**, 30843–30848
- Li, B.-L., Li, X.-L., Duan, Z.-J., Lee, O., Lin, S., Ma, Z.-M., Chang, C. C. Y., Yang, X.-Y., Park, J. P., Mohandas, T. K., Noll, W., Chan, L., and Chang, T.-Y. (1999) *J. Biol. Chem.* **274**, 11060–11071
- Lin, S., Cheng, D., Liu, M.-S., Chen, J., and Chang, T.-Y. (1999) *J. Biol. Chem.* **274**, 23276–23285
- Fujimura, K., Ise, N., Ueno, E., Hori, T., Fujii, N., and Okada, M. (1997) *J. Clin. Lab. Anal.* **11**, 315–322
- Harlow, E., and Lane, D. (1988) *Antibodies: A Laboratory Manual*, Cold Spring Harbor Laboratory, Cold Spring Harbor, NY
- Folch, J., Lees, M., and Sloane Stanley, G. A. (1957) *J. Biol. Chem.* **226**, 497–509
- Heider, J., and Boyett, R. L. (1978) *J. Lipid. Res.* **19**, 514–518
- Billheimer, J. T., Tavani, D., and Nes, W. R. (1981) *Anal. Biochem.* **111**, 331–335
- Becker, A., Bottcher, A., Lackner, K. J., Fehring, P., Notka, F., Aslanidis, C., and Schmitz, G. (1994) *Arterioscler. Thromb.* **14**, 1346–1355
- Paigen, B., Morrow, A., Holmes, P. A., Mitchell, D., and Williams, R. A. (1987) *Atherosclerosis* **68**, 231–240
- Shimada, M., Ishibashi, S., Inaba, T., Yagyu, H., Harada, K., Osuga, J.-I., Ohashi, K., Yazaki, Y., and Yamada, N. (1996) *Proc. Natl. Acad. Sci. U. S. A.* **93**, 7242–7246
- Lee, O., Chang, C. C., Lee, W., and Chang, T. Y. (1998) *J. Lipid. Res.* **39**, 1722–1727
- Lemp, M. A., Wolfley, D. E. (1992) in *Adler's Physiology of the Eye* (Hart, W. M., ed) pp. 18–28, Mosby, St. Louis, MO
- Reindel, J. F., Dominick, M. A., Bocan, T. M., Gough, A. W., and McGuire, E. J. (1994) *Toxicol. Pathol.* **22**, 510–518
- McCulley, J. P., and Sciallis, G. F. (1977) *Am. J. Ophthalmol.* **84**, 788–793
- Jong, M. C., Gijbels, M. J. J., Dahlmans, V. E., Gorp, P. J., Koopman, S. J., Ponec, M., Hofker, M. H., and Havekes, L. M. (1998) *J. Clin. Invest.* **101**, 145–152
- Gates, A. H., and Karasek, M. A. (1965) *Science* **148**, 1471–1473
- Zheng, Y., Eilertsen, K. J., Ge, L., Zhang, L., Sundberg, J. P., Prouty, S. M., Stenn, K. S., and Parimoo, S. (1999) *Nat. Genet.* **23**, 268–270
- Tabas, I. (1997) *Trends Cardiovasc. Med.* **7**, 256–263
- Burgdorf, W. H. C. (1998) in *Liver's Histopathology of the Skin* (Elder, D., Elenitsas, R., Javorsky, C., and Johnson, B., Jr. eds) 8th Ed., pp. 591–616, Lippincott-Raven Publishers, Philadelphia, PA
- Krause, B. R., and Bocan, T. M. A. (1995) *ACAT Inhibitors: Physiologic Mechanisms for Hypolipidemic and Anti-atherosclerotic Activities in Experimental Animals* (Ruffolo, R. R., Jr., and Hollinger, M. A., eds) CRC Press, Boca Raton, FL
- Bocan, T. M., Mueller, S. B., Uhlendorf, P. D., Newton, R. S., and Krause, B. R. (1991) *Arterioscler. Thromb.* **11**, 1830–1843
- Accad, M., Smith, S. J., Newland, D. L., Sanan, D. A., King, L. E., Jr., Linton, M. F., Fazio, S., and Farese, R. V., Jr. (2000) *J. Clin. Invest.* **105**, 711–719